The Role of Shearwise and Transverse Quasigeostrophic Vertical Motions in the Midlatitude Cyclone Life Cycle

JONATHAN E. MARTIN

Department of Atmospheric and Oceanic Sciences, University of Wisconsin—Madison, Madison, Wisconsin

(Manuscript received 14 March 2005, in final form 25 July 2005)

ABSTRACT

The total quasigeostrophic (QG) vertical motion field is partitioned into transverse and shearwise couplets oriented parallel to, and along, the geostrophic vertical shear, respectively. The physical role played by each of these components of vertical motion in the midlatitude cyclone life cycle is then illustrated by examination of the life cycles of two recently observed cyclones.

The analysis suggests that the origin and subsequent intensification of the lower-tropospheric cyclone responds predominantly to column stretching associated with the updraft portion of the shearwise QG vertical motion, which displays a single, dominant, middle-tropospheric couplet at all stages of the cyclone life cycle. The transverse QG omega, associated with the cyclones' frontal zones, appears only after those frontal zones have been established. The absence of transverse ascent maxima and associated column stretching in the vicinity of the surface cyclone center suggests that the transverse ω plays little role in the initial development stage of the storms examined here. Near the end of the mature stage of the life cycle, however, in what appears to be a characteristic distribution, a transverse ascent maximum along the western edge of the warm frontal zone becomes superimposed with the shearwise ascent maximum that fuels continued cyclogenesis.

It is suggested that use of the shearwise/transverse diagnostic approach may provide new and/or supporting insight regarding a number of synoptic processes including the development of upper-level jet/front systems and the nature of the physical distinction between type A and type B cyclogenesis events.

1. Introduction

The midlatitude cyclone is a propagating baroclinic wave disturbance characterized by the generation, amplification, and deformation of a lower-tropospheric thermal wave. The vertical motions that accompany these storms represent an important link between their underlying dynamics and associated sensible weather, manifest in the characteristic comma-shaped cloud and precipitation distribution associated with the cyclone. Given their direct relationship to the sensible weather associated with cyclones, the distribution of cloud and precipitation features and diagnosis of their generative vertical motions have been topics of active research for many years. More than 80 yr ago, Bjerknes and Solberg (1922) provided the first insights into the nature of this distribution by drawing attention to the frontal structure of the midlatitude cyclone. They hypothesized that upgliding motions along the warm edges of both the cold and warm fronts in the cyclone produced the linear bands of cloud and precipitation associated with each of these features. Some years later, Sawyer (1956) and Eliassen (1962) provided a solid dynamical explanation for these frontal upgliding motions demonstrating that elongated couplets of vertical motion that *straddle* the geostrophic vertical shear are a direct consequence of a particular type of deformation of the lower-tropospheric thermal wave—namely, frontogenesis.

In work concerning diagnosis of surface development [i.e., the intensification of a sea level pressure (SLP) minimum], Sutcliffe (1947) demonstrated that a significant portion of the synoptic-scale vertical motion could be attributed to cyclonic vorticity advection by the thermal wind ($-\mathbf{V}_T \cdot \nabla\zeta g$). Given the nondivergence of the geostrophic wind on an f plane, this is equivalent to the flux divergence of the vector $\mathbf{V}_T\zeta_g$, which, by definition, is aligned parallel to the geostrophic vertical shear.

Corresponding author address: Dr. Jonathon E. Martin, Department of Atmospheric and Oceanic Sciences, University of Wisconsin—Madison, 1225 W. Dayton Street, Madison, WI 53706.
E-mail: jemarti1@wisc.edu

Consequently, this portion of the vertical motion is distributed in couplets aligned *along* the thermal wind vector.

In a pioneering study using output from a frictionless, *f*-plane, primitive equation channel model of the evolution of a baroclinic wave to finite amplitude, Keyser et al. (1992) examined the quasigeostrophic (QG) vertical motion in the mature and postmature phases of an idealized cyclone. They demonstrated that the total QG vertical motion is composed of two components, which they termed ω_s and ω_n.[1] The ω_s component was cellular in structure and attributed to the along-isentrope component of $\mathbf{Q}$ ($\mathbf{Q}_s$). The ω_n component was banded in structure and attributed to the across-isentrope component of $\mathbf{Q}$ ($\mathbf{Q}_n$). They concluded that the characteristic comma-shaped vertical motion distribution of the midlatitude cyclone arises from a modification of the cellular (ω_s) dipole pattern by the banded (ω_n) dipoles associated with frontal zones. Changes in the magnitude and direction of the geostrophic vertical shear throughout the midlatitude cyclone life cycle are tied to the evolution of the cyclone's thermal structure via thermal wind balance. To emphasize their orientations relative to the thermal wind, the present study will refer to ω_s and ω_n as the shearwise (along shear) and *transverse* (across shear) QG vertical motions, respectively.

Synoptic experience supports the notion that the existence of these two separate components of the vertical motion field is more than an intellectual curiosity. It is often observed, for instance, that a transverse (frontal) circulation, while quite capable of producing significant sensible weather, is usually incapable of producing systematic surface development (e.g., Martin 1998). Conversely, significant surface cyclogenesis is almost always accompanied by the growth of the "cloud head" portion of the comma cloud structure (e.g., Reed and Albright 1986; Bader et al. 1995) whose morphology is often unrelated to the evolving frontal structure. Such observations suggest that the transverse and shearwise vertical motions may play fundamentally different roles in the life cycle of the midlatitude cyclone.

Such a suggestion is consistent with simple theoretical expectations concerning the likely cyclogenetic influences of these two components of vertical motion. According to the QG vorticity equation, any local maximum in upward vertical motion promotes an increase in geostrophic relative vorticity (via column stretching) and, thus, geopotential height or pressure falls as well. It is fairly clear, however, that the distribution of such upward vertical motion maxima with respect to the thermal wind vector determines their cyclogenetic potency to a large degree. For instance, a solitary, purely transverse, thermally direct vertical motion couplet will produce opposing bands of positive and negative vorticity on the warm and cold sides of the associated baroclinic zone as shown in Fig. 1a. Note that none of the hypothesized meridional flow (thin arrows) associated with the intensified circulation will advect temperature in such a way as to promote creation of a thermal wave.[2] A purely shearwise vertical motion couplet, on the other hand, is clearly associated with the development of a thermal wave through column stretching and attendant vorticity production (Fig. 1b). Such a thermal wave is an essential component of the cyclogenetic environment as viewed from either the QG height tendency (Holton 1992) or potential vorticity (PV; Hoskins et al. 1985) perspectives. Thus, theory supports the notion that shearwise ascent is inherently and consistently associated with cyclogenesis.

The purpose of this paper is to consider the validity of this suggestion by means of examining the evolutions of the separate shearwise and transverse QG vertical motions throughout the life cycles of two observed midlatitude cyclones. The paper is structured in the following way. In section 2 a review of the decomposition of the QG vertical motion field into its separate shearwise and transverse components is given. A synoptic description of the two example cyclone life cycles is offered in section 3. In section 4, the separate shearwise and transverse components of the vertical motion field are traced through the life cycles of the two cyclones. Finally, a discussion of the results and some conclusions are offered in section 5.

2. Isolation of the shearwise and transverse components of the vertical motion

a. Quasigeostrophic omega equation

To separate the shearwise and transverse vertical motions, their respective dynamical forcings must be isolated. Currently, there is no such method available for partitioning the full primitive equation vertical motion field. Consequently, we shall consider only the QG vertical motion in this study. Use of the $\mathbf{Q}$ vector form of the QG omega equation provides a convenient and rigorous means to isolate the transverse and shearwise

[1] Similar reference is made to these two components of QG vertical motion by Pyle et al. (2004) in their study of jet streaks.

[2] The isobaric thermal advection by the secondary circulations implied in Figs. 1a and 1b is *not* included in the QG framework. Thus, the conceptual basis for Fig. 1 is conjectural.

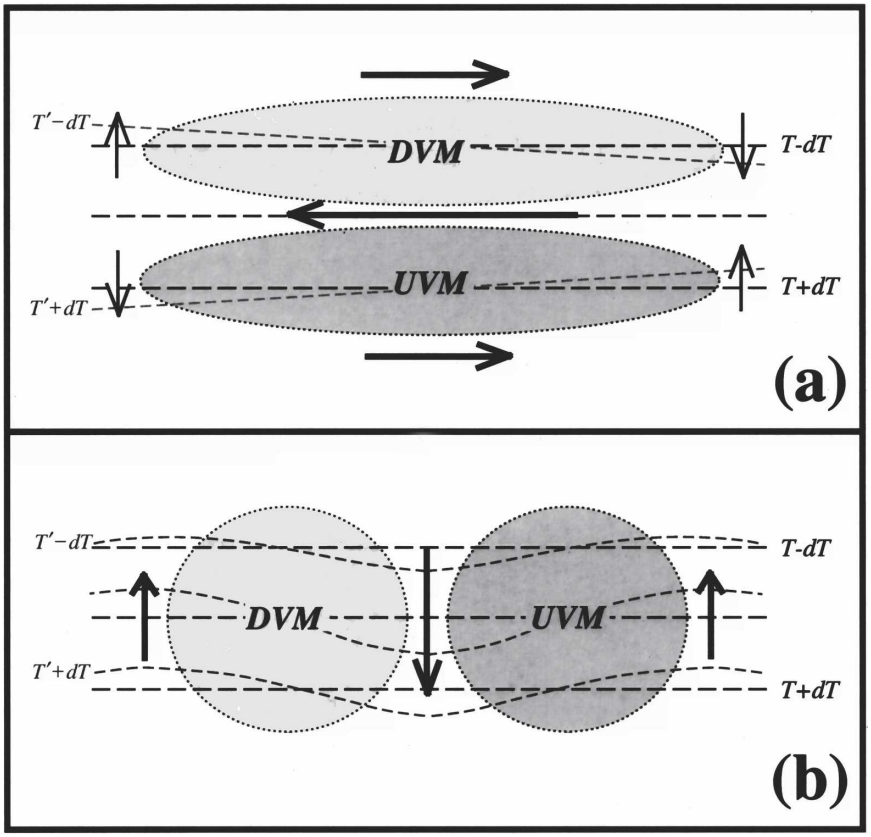

FIG. 1. (a) Effect of a purely transverse, thermally direct vertical circulation on a zonally oriented baroclinic zone. Dashed black lines are isotherms at some initial time. Dark (light) shading represents upward (downward) vertical motion [UVM (DVM)]. UVM (DVM) produces cyclonic (anticyclonic) vorticity tendencies, and bold black arrows represent the induced horizontal winds. Light gray dashed lines represent the isotherms after exposure to the induced circulation. Lighter arrows represent the induced circulations at the ends of linear bands of ascent and descent. (b) Effect of a shearwise vertical motion couplet on a zonally oriented baroclinic zone. UVM and DVM regions, initial and final isotherms, and induced circulations indicated as in (a). Note how the induced circulation produces a thermal wave only in the case of shearwise vertical motions.

components of the QG vertical motion. Following Hoskins et al. (1978), the QG omega equation can be written as

$$\left(\sigma\nabla^2 + f_o^2\frac{\partial^2}{\partial p^2}\right)\omega = -2\nabla\cdot\mathbf{Q}, \qquad (1)$$

where $\mathbf{Q}$ is defined as

$$\mathbf{Q} = -f_o\gamma\left[\left(\frac{\partial\mathbf{V}_g}{\partial x}\cdot\nabla\theta\right)\mathbf{i} + \left(\frac{\partial\mathbf{V}_g}{\partial y}\cdot\nabla\theta\right)\mathbf{j}\right], \qquad (2)$$

with $\gamma = (R/f_o p_o)(p_o/p)^{(c_v/c_p)}$. The static stability, σ, is given by $\sigma = -(RT_o/p\theta_o)(\partial\theta_o/\partial p)$, where T_o and θ_o are the domain-averaged temperature and potential temperature at each level, respectively. For adiabatic, geo-

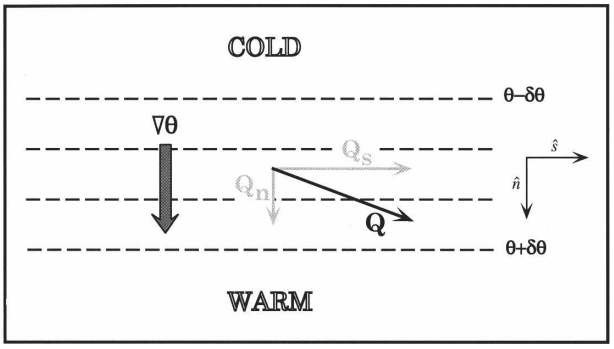

FIG. 2. Schematic describing the natural coordinate partitioning of the $\mathbf{Q}$ vector used in this study. Thick dashed lines are isentropes on an isobaric surface. Q_n (Q_s) is the component of $\mathbf{Q}$ is the $\mathbf{n}$ ($\mathbf{s}$) direction, and its divergence is associated with transverse (shearwise) QG vertical motion.

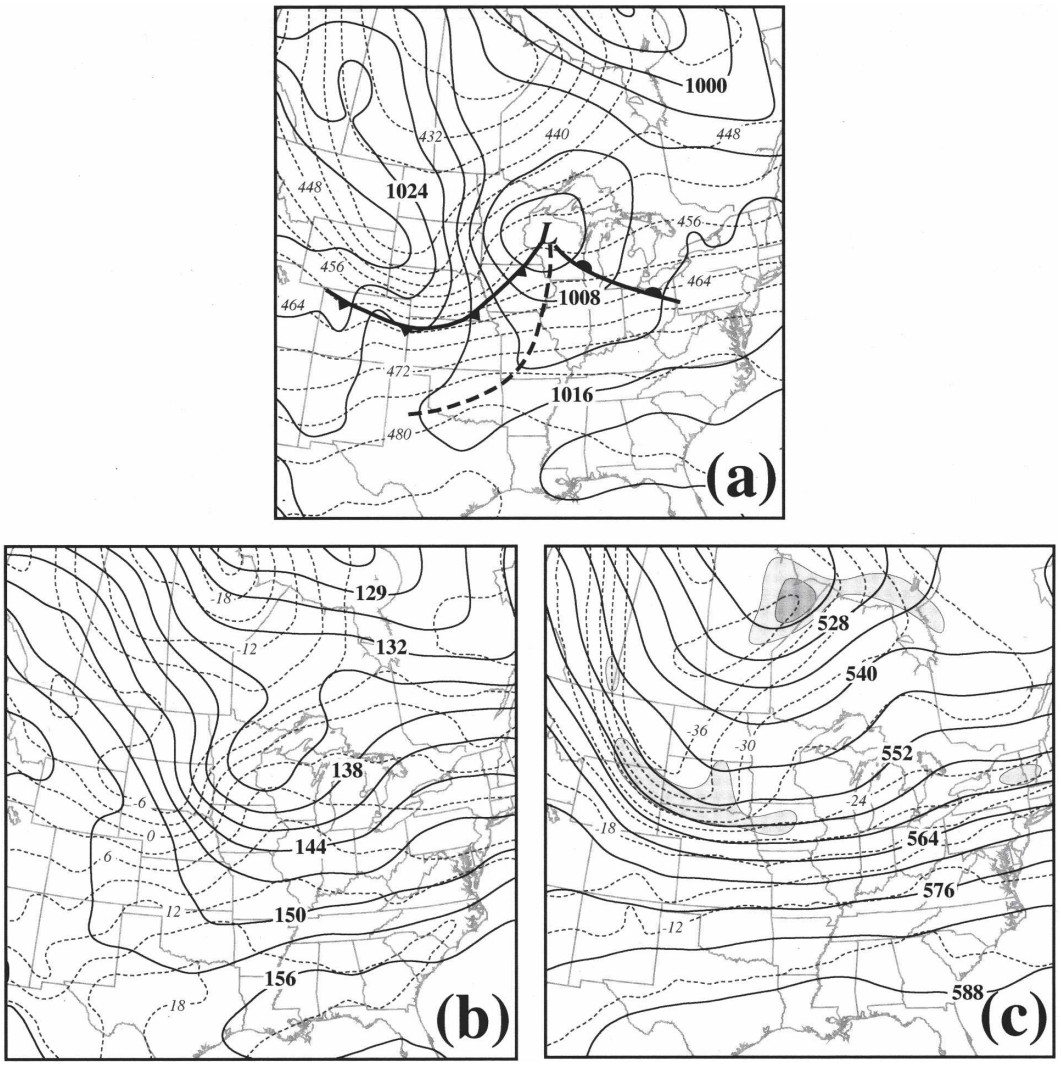

FIG. 3. (a) SLP and 900–500 hPa thickness analyses from the 0-h forecast of the NCEP Eta model valid at 1200 UTC 12 Nov 2003. Solid lines are sea level isobars labeled in hPa and contoured every 4 hPa. Dashed lines are 900–500 hPa thickness isopleths labeled in dam and contoured every 4 dam. Conventional frontal symbols mark the surface cold and warm fronts. Thick dashed line is a leeside trough and "L" indicates location of the SLP minimum. (b) 850 hPa geopotential and temperature analyses from the 0-h forecast of the NCEP Eta model valid at 1200 UTC 12 Nov 2003. Solid lines are geopotential heights labeled in dam and contoured every 3 dam. Dashed lines are isotherms labeled in °C and contoured every 3°C. (c) 500-hPa geopotential, temperature, and absolute vorticity analyses from the 0-h forecast of the NCEP Eta model valid at 1200 UTC 12 Nov 2003. Solid lines are geopotential heights labeled in dam and contoured every 6 dam. Dashed lines are isotherms labeled in °C and contoured every 3°C. Absolute vorticity is shaded in units of 10^{-5} s^{-1} and contoured every 5×10^{-5} s^{-1} beginning at 20×10^{-5} s^{-1}.

strophic flow the **Q** vector represents the rate of change of the vector $\nabla_p\theta$ following the geostrophic wind;

$$\mathbf{Q} = f_o\gamma \frac{d}{dt_g}\nabla_p\theta, \tag{3}$$

where $d/dt_g = \partial/\partial p + \mathbf{V}_g \cdot \nabla_p$ (the subscript g denotes geostrophic). Thus, the **Q** vector contains information about the rate of change of both the *magnitude* and *direction* of $\nabla_p\theta$. As shown in Fig. 2, for any arbitrary **Q** vector, only the component of **Q** *perpendicular* to the isentropes ($\mathbf{Q}_n$) can change the magnitude of $\nabla_p\theta$ while only the component *parallel* to the isentropes ($\mathbf{Q}_p$) can change the direction of $\nabla_p\theta$. The present vector decomposition of **Q** into components along the direction of the potential temperature gradient vector (**n**) and 90° counterclockwise from that direction (**s**, $\mathbf{s} = \mathbf{k} \times \mathbf{n}$) follows that outlined in Martin (1999a) and is illustrated

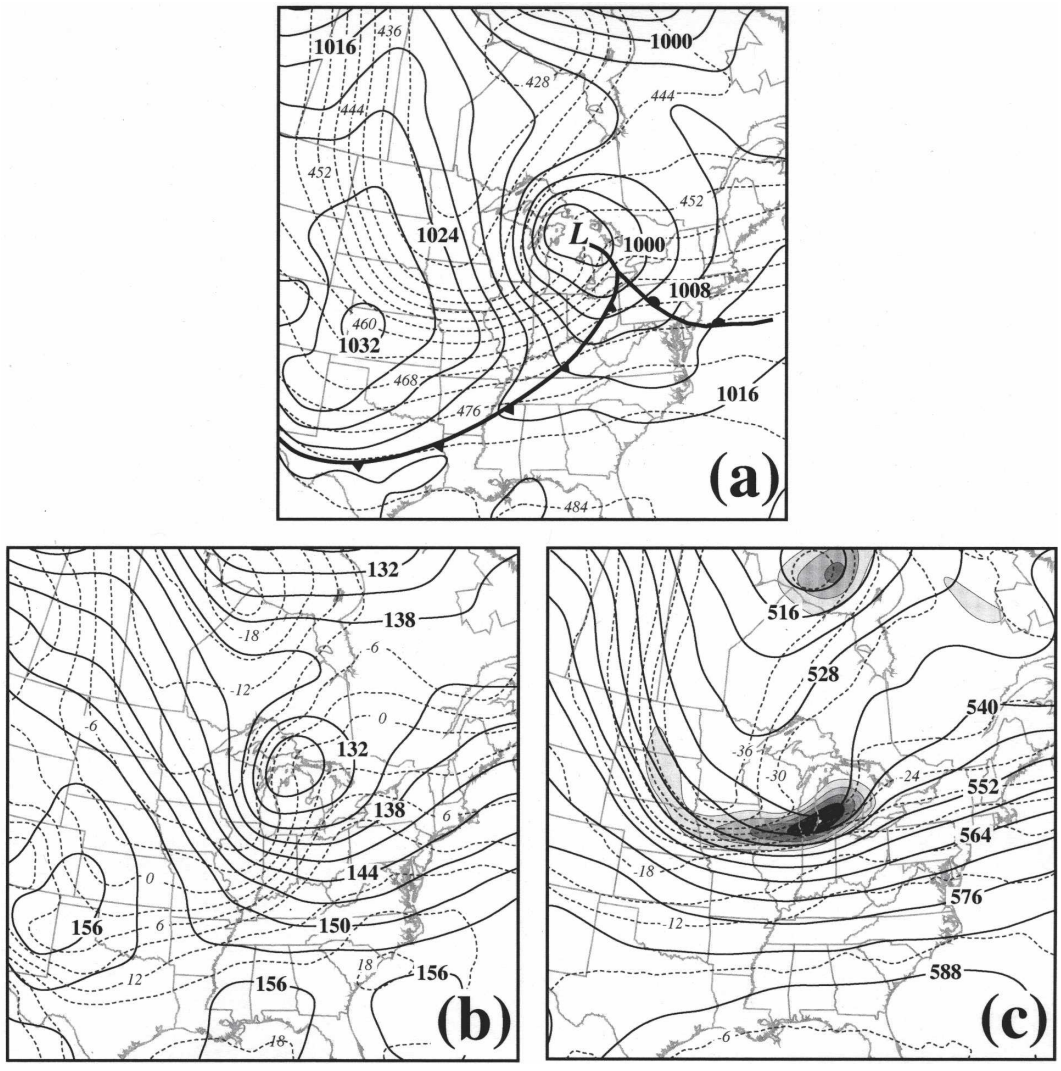

FIG. 4. Same as in Fig. 3, but for 0000 UTC 13 Nov 2003.

with the aid of Fig. 2. The unit vector in the direction of $\nabla\theta$ is given by

$$\mathbf{n} = \frac{\nabla\theta}{|\nabla\theta|}. \tag{4}$$

The component of $\mathbf{Q}$ in the direction of $\mathbf{n}$ will be denoted as Q_n and is equal to

$$\mathbf{Q}_n = \left(\frac{\mathbf{Q}\cdot\nabla\theta}{|\nabla\theta|}\right)\frac{\nabla\theta}{|\nabla\theta|} \quad \text{or} \quad \mathbf{Q}_n = \left(\frac{\mathbf{Q}\cdot\nabla\theta}{|\nabla\theta|}\right)\mathbf{n}. \tag{5}$$

Recalling that the QG frontogenesis function is given by $F_g = (\mathbf{Q}\cdot\nabla\theta)/|\nabla\theta|$ (Hoskins and Pedder 1980), the expression for $\mathbf{Q}_n$ reduces to $\mathbf{Q}_n = -F_g\mathbf{n}$. Thus, $\mathbf{Q}_n$ is large (*small*) where F_g is large (*small*). By virtue of the defining orientation of the $\mathbf{Q}_n$ vectors to isotherms, the QG forcing of vertical motion associated with $\mathbf{Q}_n$ (i.e., $-2\nabla\cdot\mathbf{Q}_n$) forces elongated, banded regions of vertical motion that are parallel to, and associated with, regions of concentrated baroclinicity (frontal zones) within the flow (Keyser et al. 1992). In other words, the across-isentrope component of $\mathbf{Q}$ relates to the forcing of transverse vertical motions that are uniquely associated with frontogenetic and frontolytic processes.

The component of $\mathbf{Q}$ along the isentropes will be denoted as $\mathbf{Q}_s$ and is equal to

$$\mathbf{Q}_s = \frac{\mathbf{Q}\cdot(\mathbf{k}\times\nabla\theta)}{|\nabla\theta|}\left[\frac{(\mathbf{k}\times\nabla\theta)}{|\nabla\theta|}\right]. \tag{6}$$

Keyser et al. (1988) demonstrated that, following the geostrophic flow, the potential temperature gradient

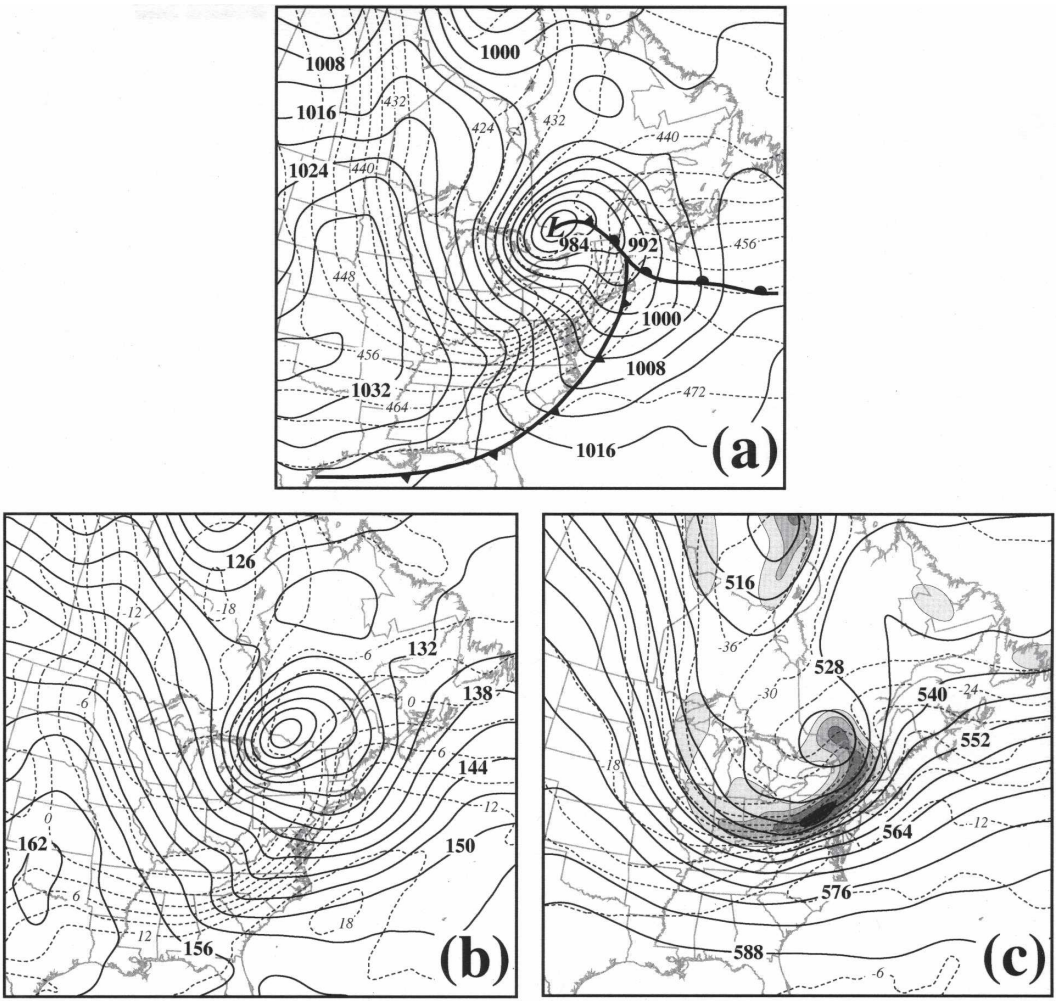

FIG. 5. Same as in Fig. 3, but for 1200 UTC 13 Nov 2003.

vector is rotated in the direction of $\mathbf{Q}_s$ to a degree proportional to the magnitude of $\mathbf{Q}_s$ (the reader is referred to that work for the complete derivation of this relationship). Keyser et al. (1992) found that the pattern of vertical motion associated with $-2\nabla \cdot \mathbf{Q}_s$ was cellular and distributed on the synoptic scale (which they termed *wave scale*). A similar result was reported by Kurz (1992). By virtue of the orientation of $\mathbf{Q}_s$ vectors to the isentropes, the resulting vertical motion couplets are distributed along, or shearwise to, the thermal wind. Therefore, a precise partitioning of the total QG omega into shearwise and transverse components is possible by separately considering the divergence of the $\mathbf{Q}_s$ and $\mathbf{Q}_n$ components of $\mathbf{Q}$, respectively. Throughout the remainder of this paper the shearwise vertical motion will be understood to be associated with $-2\nabla \cdot \mathbf{Q}_s$, while the transverse vertical motion will be understood to be associated with $-2\nabla \cdot \mathbf{Q}_n$.

b. Calculation of QG omega

In the subsequent analysis, gridded model output from the National Centers for Environmental Prediction's (NCEP's) Eta and Global Forecast System (GFS) models is used in the calculation of the QG omega. These gridded data are first bilinearly interpolated from their original output grid to a 1° × 1° latitude–longitude grid at 12 isobaric levels (1000, 900, 800, 700, 600, 500, 400, 300, 250, 200, 150, and 100 hPa) using an interpolation program included in the General Meteorology Package (GEMPAK). Employing the technique of successive over relaxation (SOR), we then solve the *f*-plane version of the QG omega equation using a spatially averaged static stability that varies for each time with f_o set equal to the central latitude (45.5°N) of the domain for each of the two cases we examine. With geostrophic forcing corresponding to the divergences of

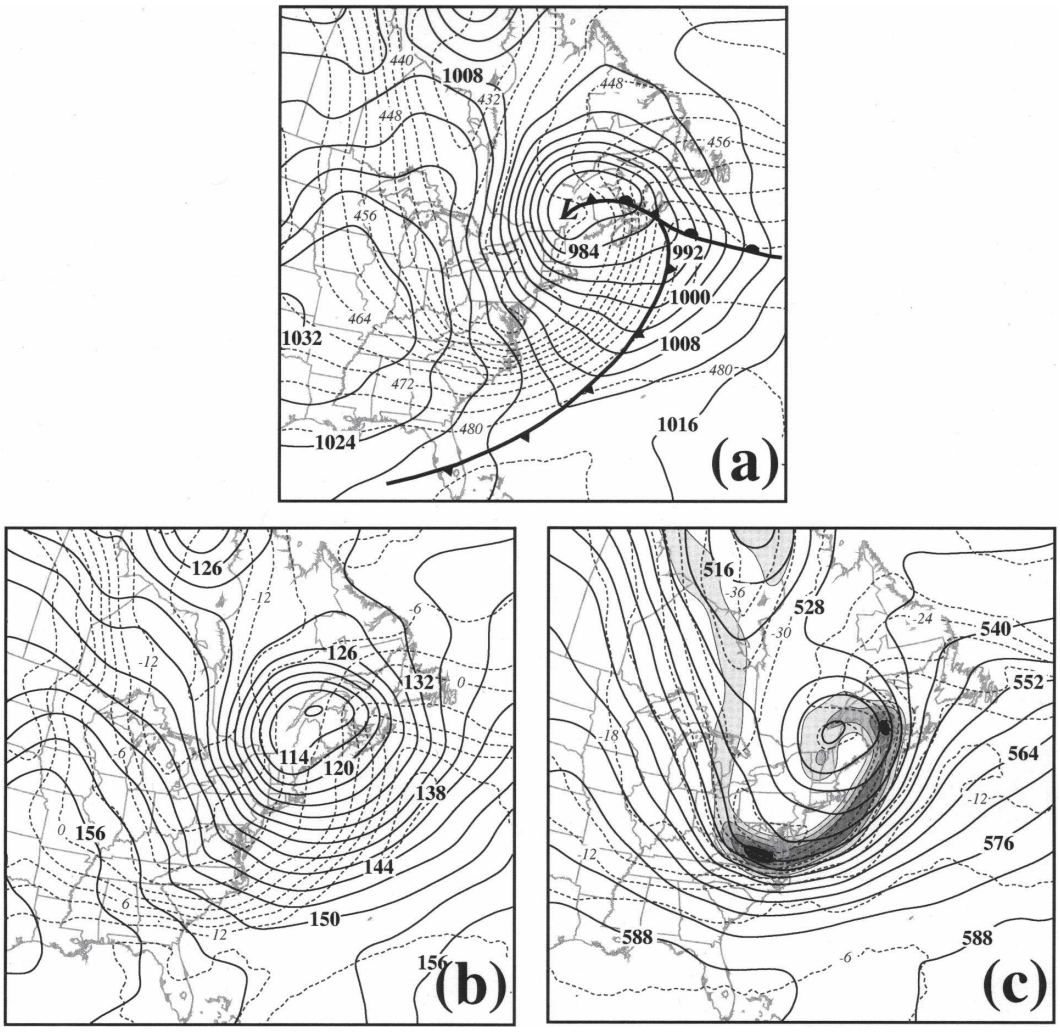

FIG. 6. Same as in Fig. 3, but for 0000 UTC 14 Nov 2003.

Q, $\mathbf{Q}_n$, and $\mathbf{Q}_s$, the total, transverse, and shearwise QG vertical motions, respectively, are returned in units of Pa s^{-1}. In the next section we present a brief synoptic overview of two observed cyclones before tracing the evolution of the separate modes of QG vertical motion throughout the life cycle of these storms.

3. Synoptic description of two case studies

a. The 12–14 November 2003 cyclone

On 11 November 2003, a weak Alberta Clipper was responsible for distributing heavy snows in portions of western Canada. From 12–14 November, that initially weak storm underwent vigorous and prolonged cyclogenesis over the northern United States. During that 48-h period, the storm deepened explosively (1.11 bergerons from 1200 UTC 12 November to 1200 UTC 13 November) and traversed the Upper Great Lakes states in association with the migration of an intense upper-level front over the same region.

At 0000 UTC 12 November a local minimum in SLP was located along the Montana/North Dakota border to the north of a rather featureless lower-tropospheric baroclinic zone spanning the eastern two-thirds of the United States (not shown). By 1200 UTC 12 November, the surface cyclone had intensified slightly while migrating eastward to northwestern Wisconsin (Fig. 3a). An intense lower-tropospheric thermal contrast had developed by this time as evidenced by the 900–500 hPa thickness (Fig. 3a) as well as the substantial temperature gradient at 850 hPa (Fig. 3b). During this same interval, an upper-tropospheric baroclinic zone that extended from central Iowa to northern Alberta had also intensified (Fig. 3c).

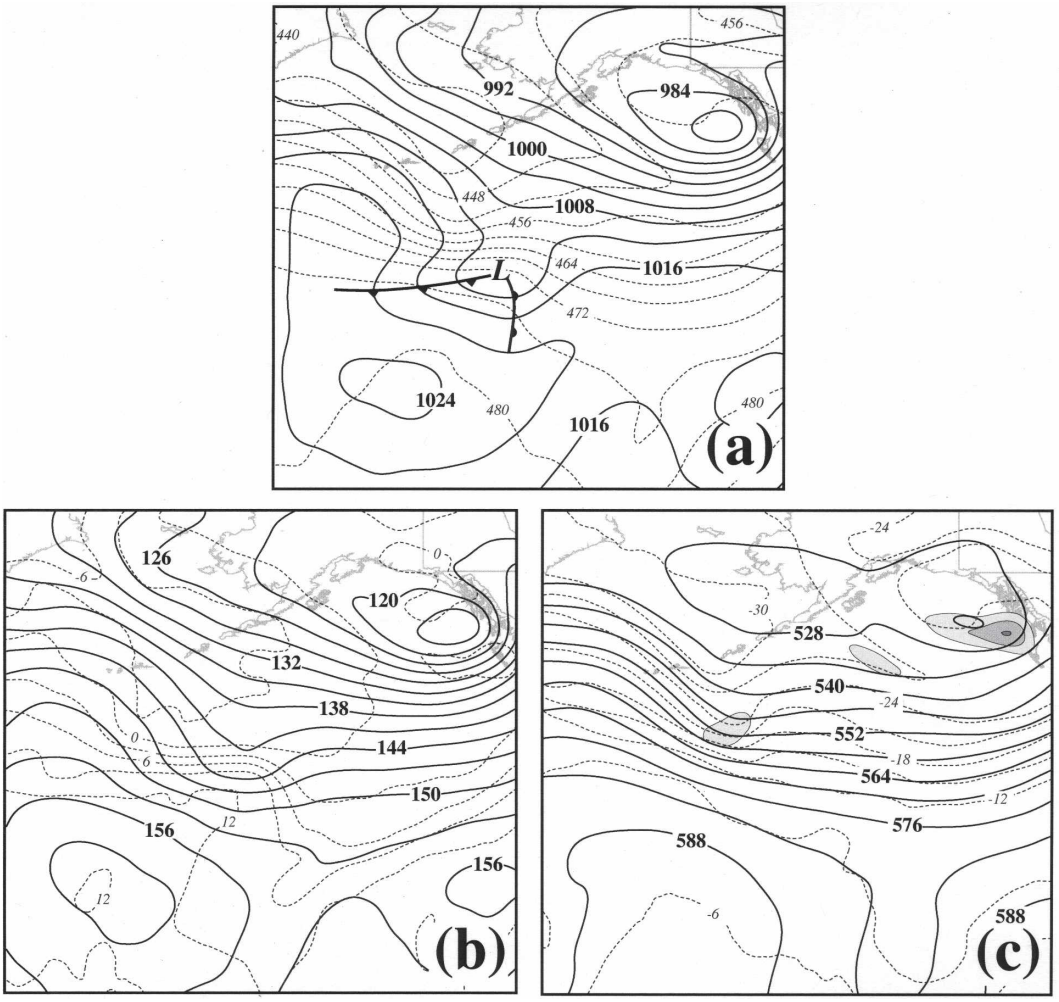

FIG. 7. Same as in Fig. 3, but from the NCEP GFS analysis valid at 1200 UTC 6 Oct 2004.

Further surface development occurred in the 12 h ending at 0000 UTC 13 November, at which time the surface cyclone center was located near Sault St. Marie, Michigan, and had a well-developed cold front stretching southwestward to central Texas (Fig. 4a). At 850 hPa, a strong cold frontal signature was clearly evident, whereas a weaker warm frontal temperature contrast attended by a diffluent geostrophic wind field suggested modest frontogenesis over the eastern Great Lakes (Fig. 4b). The upper-level front had greatly intensified by this time as it exhibited a 12°C temperature contrast at 500 hPa over approximately 225 km above central Iowa (Fig. 4c). A potent upper-tropospheric short wave had also developed by this time at the eastern end of the upper frontal baroclinic zone over central lower Michigan as evidenced by the 500-hPa absolute vorticity (Fig. 4c).

In association with the continued intensification of the upper-tropospheric wave, the surface cyclone also continued to strengthen, reaching an SLP minimum of 981 hPa by 1200 UTC 13 November (Fig. 5a). The cyclone appeared occluded by this time as the SLP minimum was disconnected from the peak of the warm sector. A deep, coherent cold frontal structure also characterized the storm at this time as evidenced by the 900–500 hPa thickness (Fig. 5a), as well as the 850- and 500-hPa potential temperatures (Figs. 5b and 5c). The primary upper-level low center was well defined at this time and the upper front had maintained its considerable intensity while continuing its eastward migration (Fig. 5c). Evidence of the occluded thermal ridge appeared in the 900–500 hPa thickness as well as the temperature fields at both 850 and 500 hPa.

Finally, at 0000 UTC 14 November, the cyclone, having undergone some reorganization in the intervening 12 h, was located over northwestern Maine and had deepened slightly further to 977 hPa. The frontal structure remained robust along the cold front (Figs. 6a and

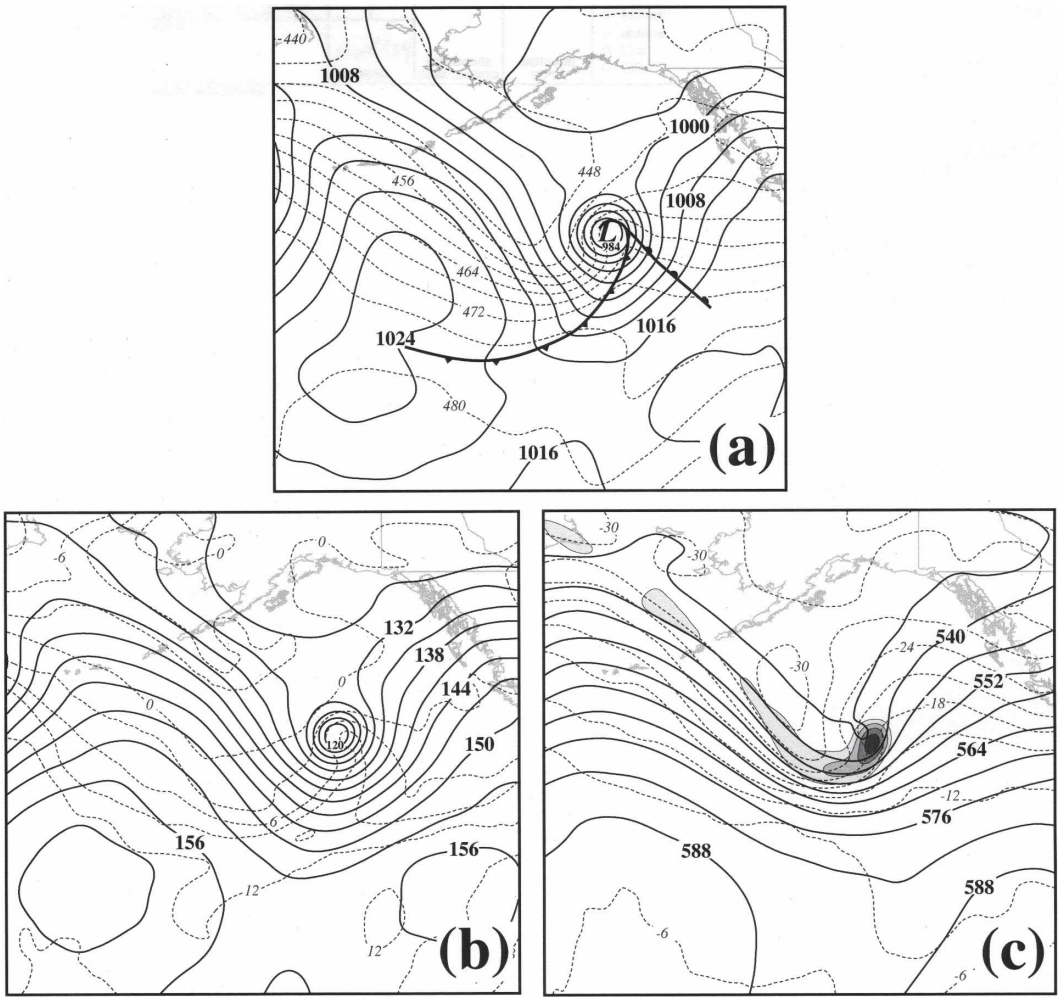

FIG. 8. Same as in Fig. 7, but for 0600 UTC 7 Oct 2004.

6b), and a better-defined warm front and thermal ridge connecting the geopotential height minimum to the peak of warm sector were evident at 850 hPa (Fig. 6b). A similar thermal ridge signature, displaced to the north of its counterpart at 850 hPa, was also evident at 500 hPa where the upper shortwave was now embedded within a negatively tilted larger-scale trough (Fig. 6c).

b. The 6–8 October 2004 cyclone

At 1200 UTC 6 October 2004 a weak surface cyclone with a central SLP of 1010 hPa was located well south of the Aleutian Islands (Fig. 7a). The baroclinic zone along which this cyclone was developing was sharply defined both in the 900–500 hPa thickness field and the 850 hPa isotherms (Fig. 7b) at which level a weak but discernible geopotential height trough was clearly evident. At 500 hPa, a shortwave embedded in general northwesterly flow was characterized by a well-developed thermal perturbation (Fig. 7c).

By 0000 UTC 7 October 2004, the surface cyclone had progressed eastward and deepened dramatically to 995 hPa (not shown). Additional rapid deepening left the SLP minimum at 982 hPa by 0600 UTC 7 October (Fig. 8a). By this time, the cyclone also exhibited a nascent occluded thermal ridge in the 900–500 hPa thickness field. This thermal ridge structure was reflected at 850 hPa as well (Fig. 8b), where equally impressive geopotential height falls characterized the development. Continued intensification of the upper vortex, both in terms of curvature and shear vorticity, was also evident at 500 hPa (Fig. 8c), where a well-developed upper front was now located at the base of a negatively tilted, diffluent upper trough.

By 1200 UTC 7 October the central SLP of the surface cyclone had dropped to 971 hPa, and a fully de-

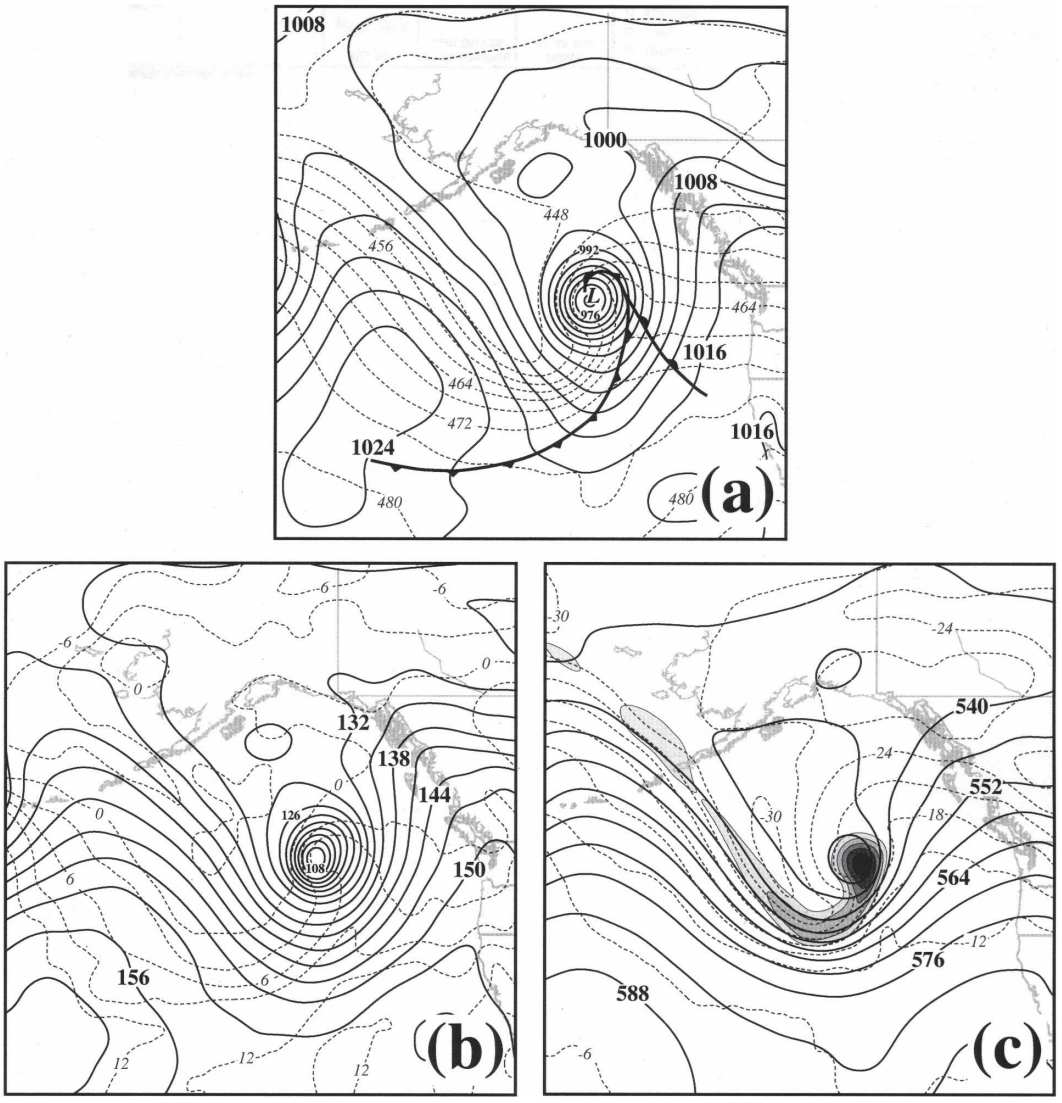

FIG. 9. Same as in Fig. 7, but for 1200 UTC 7 Oct 2004.

veloped occluded thermal structure characterized the storm not only at sea level (Fig. 9a) but also at 850 hPa (Fig. 9b), where, as before, the development was as impressive as it was at sea level. Even at 500 hPa, where the upper vortex and shortwave had further intensified, there was a hint of a thermal ridge wrapping into the geopotential height minimum (Fig. 9c).

In the 12-h period between 1200 UTC 7 October and 0000 UTC 8 October, the minimum SLP of the surface cyclone oscillated within 2 hPa of 972 hPa as the storm continued to wrap up off the Washington/British Columbia coast (Fig. 10a). The occluded thermal ridge lengthened considerably during this wrapping-up period as evidenced in the all three panels of Fig. 10. As appears to be characteristic in such wrapped-up storms, the northern and eastern edges of the vorticity maximum at 500 hPa were nicely coincident with the position of the surface cold and occluded fronts (Fig. 10c) as discussed in Martin (1998).

4. Evolution of the QG omega in the cyclone life cycles

In this section, we examine the evolution of the shearwise and transverse QG omega for the cyclones described in section 3. Though omega was available at a variety of vertical levels as described in section 2c, 700-hPa omega is most consistently representative of the distribution of vertical motions in the lower to middle troposphere throughout the life cycle, and we

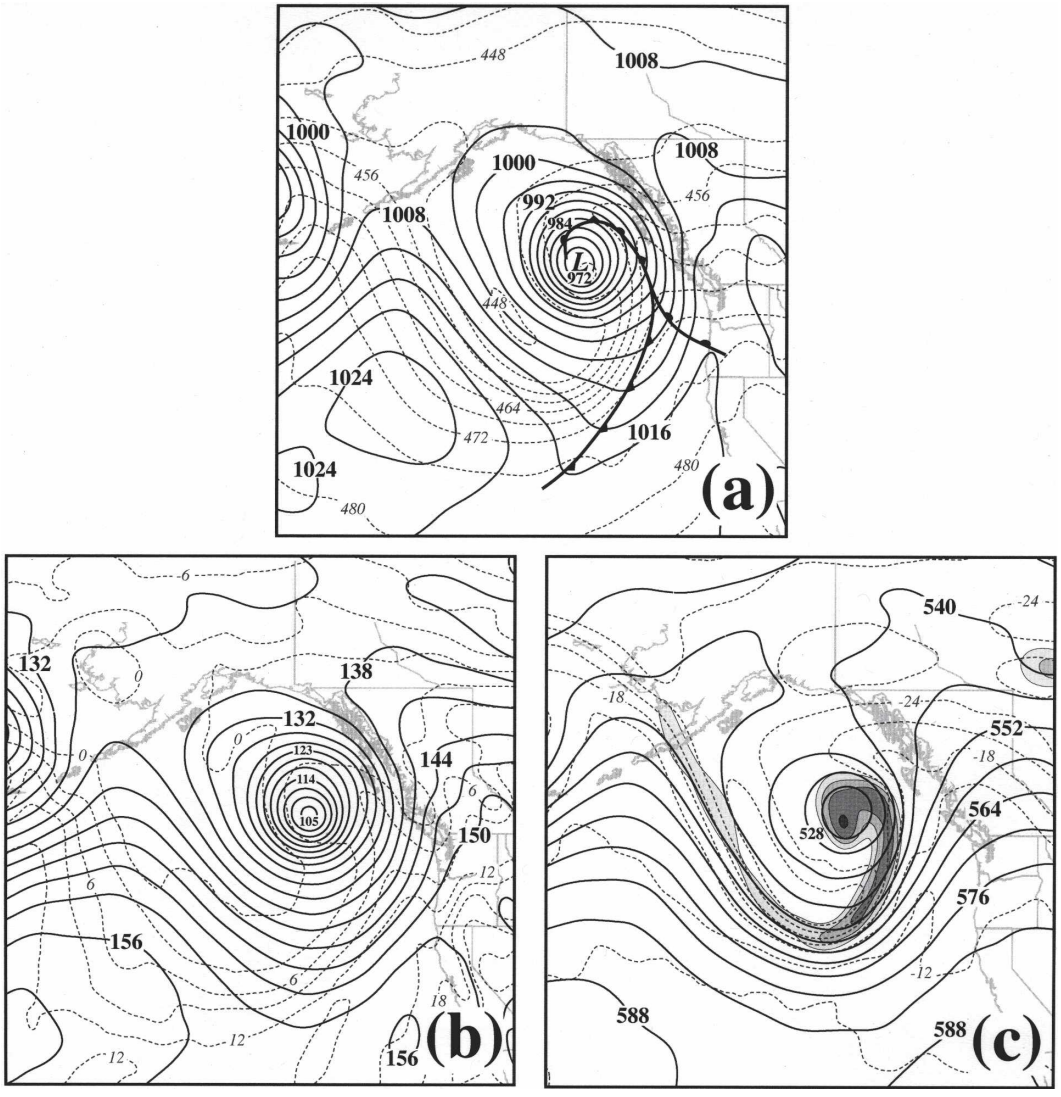

FIG. 10. Same as in Fig. 7, but for 0000 UTC 8 Oct 2004.

chose to employ 700-hPa omega in the subsequent presentation. We begin by examining the QG omega evolution in the November 2003 storm.

a. Partitioned QG omega for November 2003 case

The total 700-hPa QG vertical motion field at 1200 UTC 12 November 2003 is shown in Fig. 11a. As might be expected in association with a developing surface cyclone, a broad region of modest ascent occurs over and to the northeast of the SLP minimum while equally modest descent occurs to the west. Evidence for nascent frontal circulations is apparent in the transverse couplets associated with the cold front and less-organized warm front (Fig. 11b). The transverse vertical motions were related to regions of QG frontogenesis (not shown) as expected. At this early stage in development, however, the essential character of the cyclone's vertical motion field is better represented by the shearwise vertical motions (Fig. 11c).

The distribution is rather similar at 0000 UTC 13 November at which time a much more robust couplet of vertical motion characterizes the cyclone (Fig. 12a) with the greatest ascent nearly directly above the SLP minimum. The cold frontal circulation had intensified by this time, as had that associated with the baroclinic zone centered over the Upper Peninsula of Michigan (Fig. 12b). Both of these locations were local maxima in geostrophic frontogenesis (not shown). Evidence for a quadrapole distribution of omega around the upper-

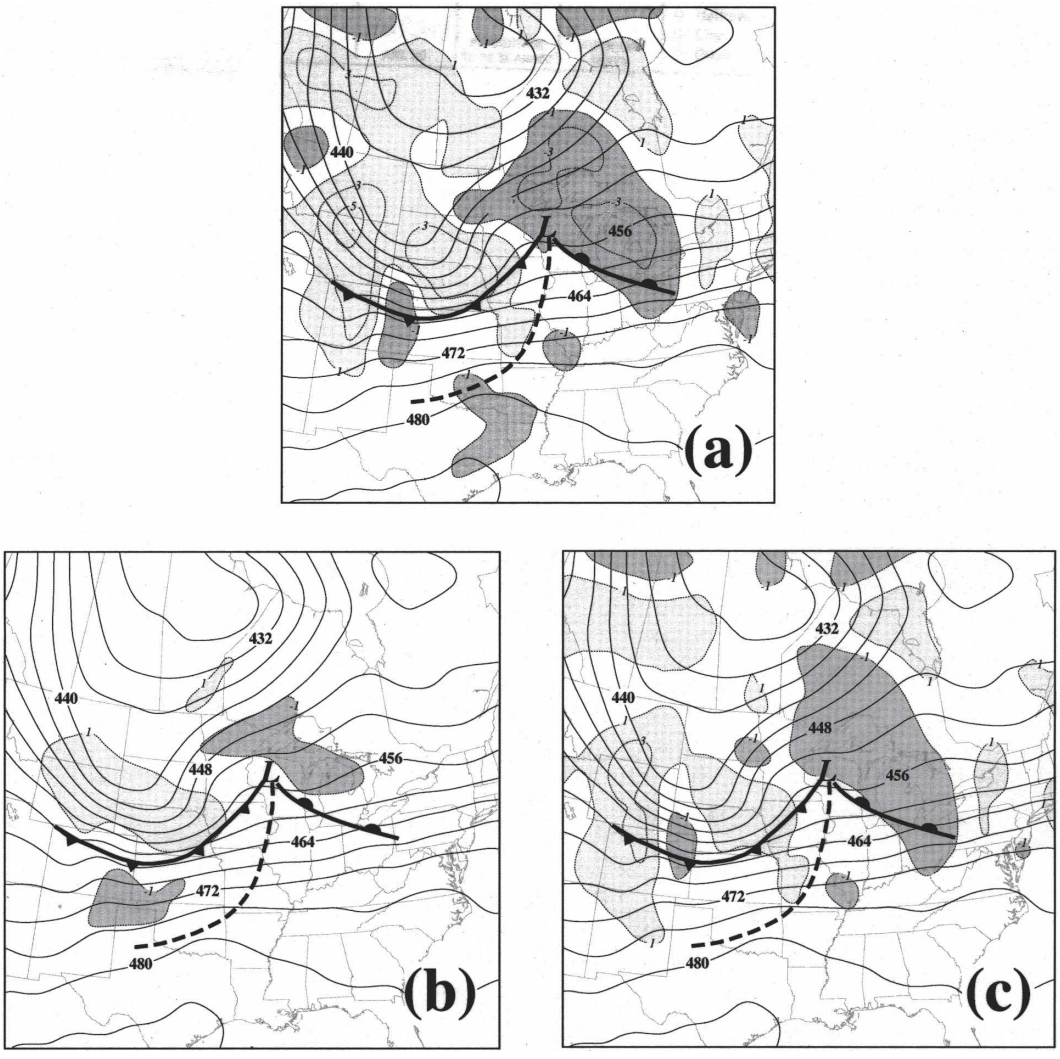

FIG. 11. (a) Total 700-hPa QG omega and 900–500 hPa thickness derived from the NCEP Eta model analysis valid at 1200 UTC 12 Nov 2003. Dark (light) shading is negative (positive) omega labeled in dPa s^{-1} and contoured every −2 (2) dPa s^{-1} starting at −1 (1) dPa s^{-1}. The 900–500 hPa thickness (thin solid lines) is labeled in dam and contoured every 4 dam. Frontal symbols and "L" indicate surface frontal positions and location of the SLP minimum, respectively. (b) Same as in (a), but for 700-hPa transverse QG omega at 1200 UTC 12 Nov 2003. (c) Same as in (a), but for 700-hPa shearwise QG omega at 1200 UTC 12 Nov 2003.

level jet/front feature, albeit with a weak right exit region component, also appears in the transverse vertical motion field from Lake Erie to western Nebraska. Once again, however, the predominant component of QG vertical motion was the solitary shearwise couplet whose ascent branch was located directly above the SLP minimum (Fig. 12c).

By 0000 UTC 14 November, a more highly amplified distribution of stronger QG vertical motions was evident in association with this developing storm (Fig. 13a). Note that, at this time, the maximum QG ascent in the cloud head portion of the cyclone was aligned along a narrow band roughly parallel to the 900:500 hPa thickness ridge axis with the SLP minimum located slightly southwest of the maximum. The transverse omega field also displays a number of interesting characteristics (Fig. 13b). First, a strong cold frontal circulation is particularly evident over the southern Appalachians where geostrophic frontogenesis was strongest. The secondary maximum in transverse ascent, located over the Canadian Maritimes, combined with the ascent portion of the Appalachian couplet forms a coherent band of ascent associated with the cold front. It appears that the northern piece is associated with the

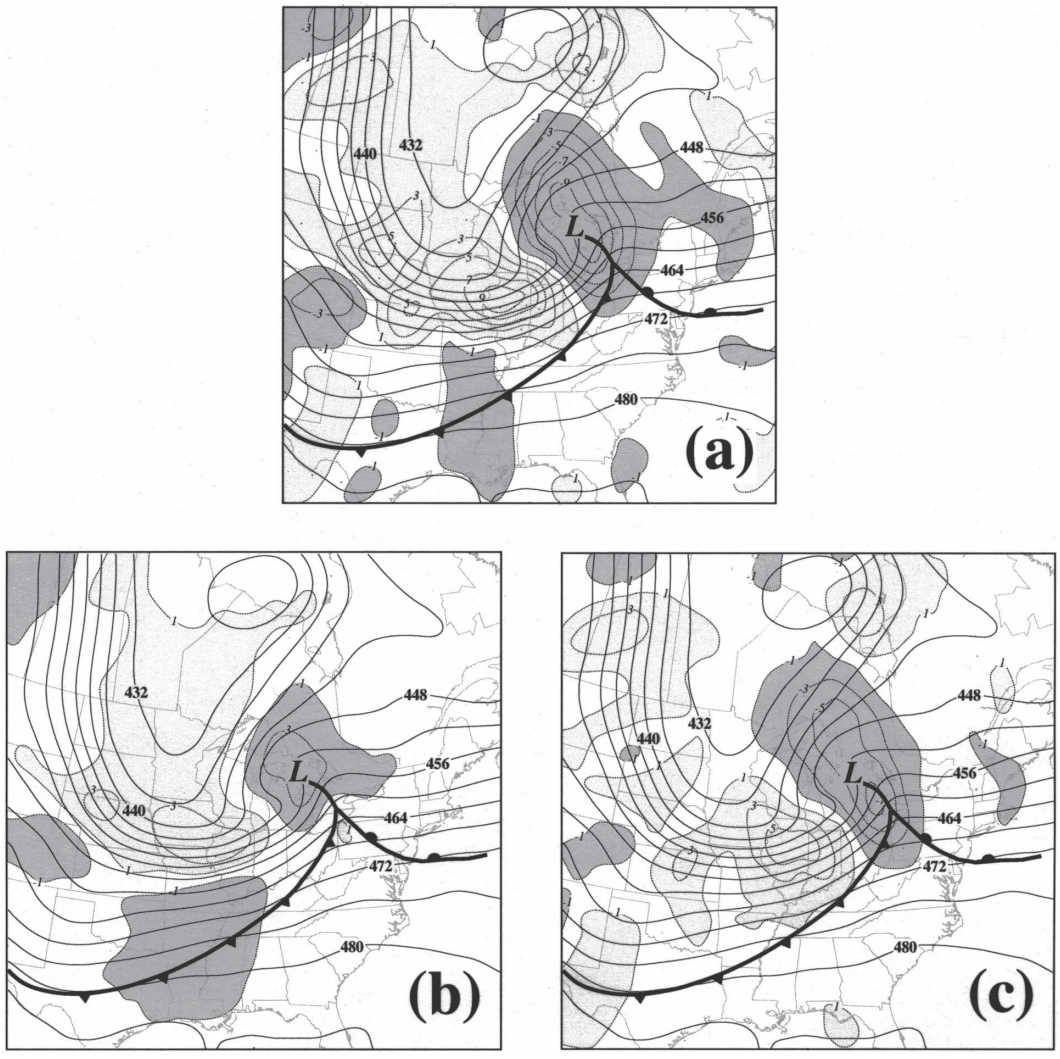

FIG. 12. Same as in Fig. 11, but for 0000 UTC 13 Nov 2003.

cold front aloft portion of the robust warm occluded thermal structure exhibited by this storm at this time. Though the shearwise vertical motions are still characterized by a single, dominant couplet with ascent over Quebec and the Maritime Provinces and descent concentrated to the southwest over eastern Kentucky (Fig. 13c), a couple of characteristics of that couplet are different at this stage in the life cycle as compared to prior stages.[3] First, the SLP minimum is not directly beneath the maximum in ascent. Second, the ascent is dominated by a narrow band of large vertical motions aligned nearly along the 900–500 hPa thickness ridge, rather abruptly ending at the peak of the warm sector.

b. Partitioned QG omega for October 2004 case

At 1200 UTC 6 October, a modest couplet of QG vertical motion straddled the trough in the 900–500 hPa thickness (Fig. 14a). As might be expected in association with a developing surface cyclone, the ascent occurred over and to the northeast of the surface cyclone while the slightly stronger descent occurred to the west. Very little evidence for frontal circulations is evident in the transverse component of the QG omega (Fig. 14b) at this time as almost no geostrophic frontogenesis was

[3] The QG ω field appears to be more structured than the flow itself in Fig. 13c. Since **Q** is the product of derivatives of the thermal and geostrophic momentum fields, each of which has a wavelike character, the multiplication of the two tends to halve the wavelength.

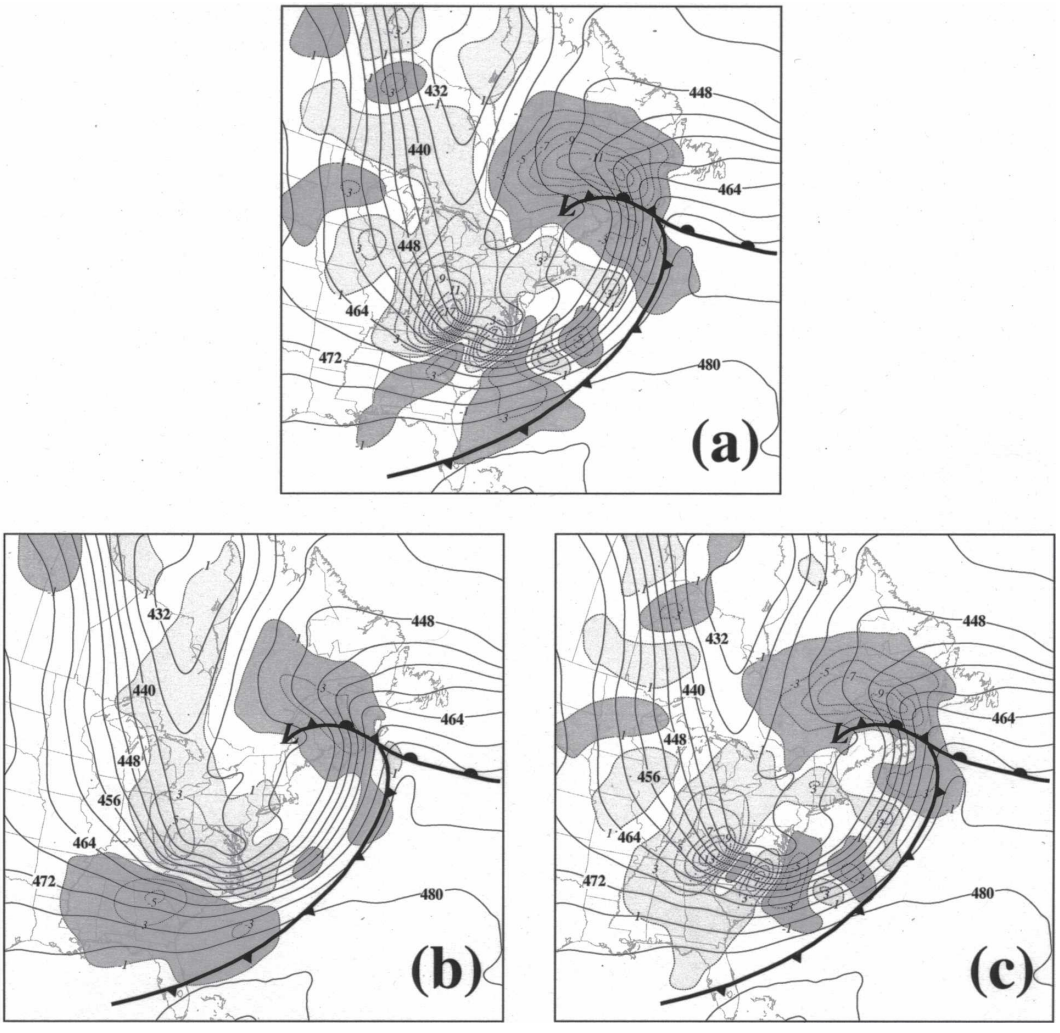

FIG. 13. Same as in Fig. 11, but for 0000 UTC 14 Nov 2003.

occurring at 700 hPa (not shown). In fact, at this nascent stage of development, the QG omega is almost entirely manifest in the shearwise couplet (Fig. 14c).

The distribution is essentially the same 12 h later when the cyclone had just entered an extended period of rapid development. The total 700-hPa QG omega displays a wavelike distribution with the ascent portion of the couplet centered just to the northeast of the surface cyclone center (Fig. 15a). The more linear descent region stretches along the cyclonic shear side of the developing upper front discussed previously. Indeed, a thermally direct transverse circulation along that baroclinic zone appears in Fig. 15b, along with a weak ascent region associated with the western edge of the developing surface warm front. The majority of the middle-tropospheric QG omega is, however, associated with the shearwise component (Fig. 15c).

Continued rapid deepening of the cyclone through 0600 UTC 7 October was coincident with a more than doubling of the 700-hPa QG omega by that time (Fig. 16a) as compared to 6 h earlier. As before, the strong ascent was located just northeast of the position of the SLP minimum. The partitioned QG omega at this time, however, revealed that the frontal circulations associated with the cyclone had become more robust with clear transverse couplets of omega associated with the elongated surface cold front and the stubbier surface warm front (Fig. 16b). Note that the ascent maximum associated with the warm frontal circulation is nearly centered on the surface cyclone center. This is related to the presence of a maximum in 700-hPa geostrophic frontogenesis directly north of the position of the surface low (not shown). Despite the clear structure evident in the transverse vertical motions, the lion's share

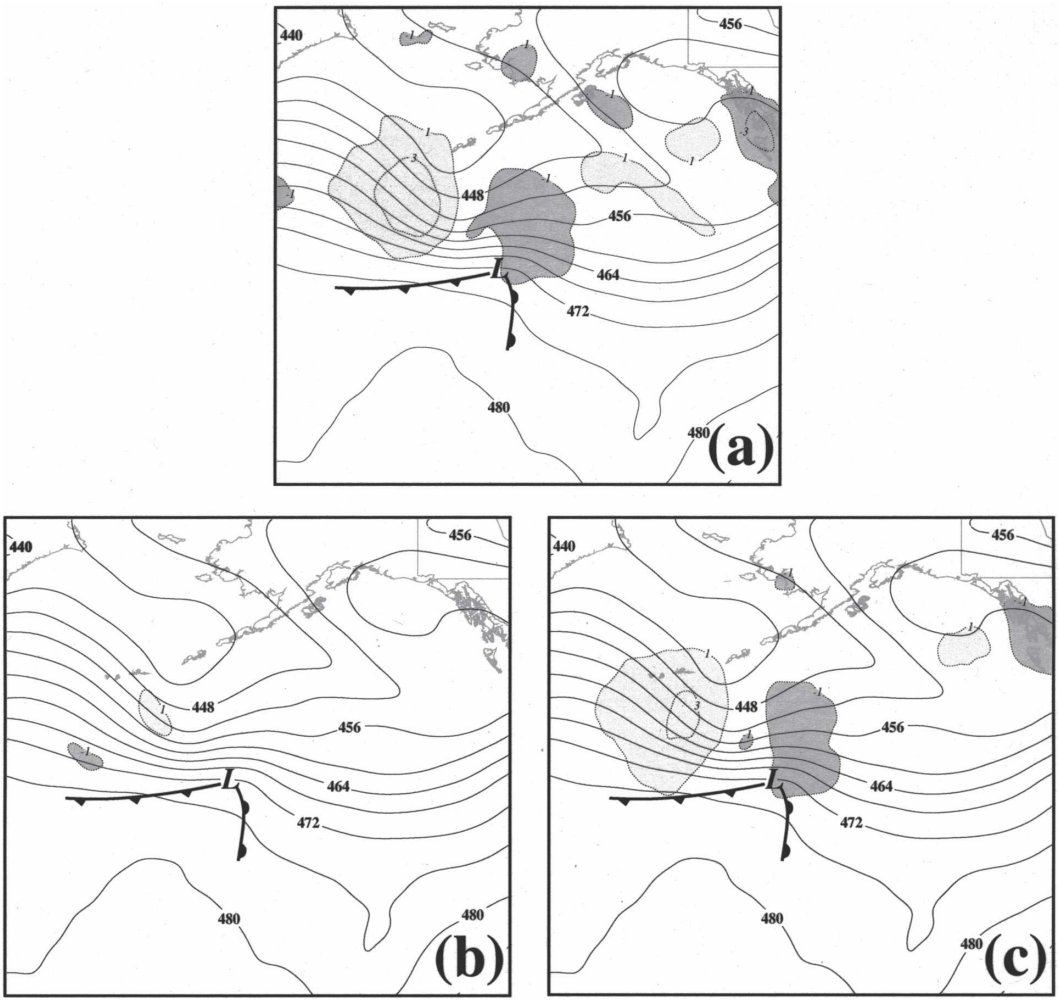

FIG. 14. Same as in Fig. 11, but derived from the NCEP GFS model analysis valid at 1200 UTC 6 Oct 2004.

of the QG omega is still contained in the shearwise component (Fig. 16c). At this time, however, the shearwise ascent maximum lies just to the *north* of the SLP minimum.

By 1200 UTC 7 October, at which time the explosive deepening was finally coming to an end, the total 700-hPa QG omega was at its most intense with the ascent (descent) maximum at -25 dPa s^{-1} (17 dPa s^{-1})(Fig. 17a). At this time, the surface cyclone was located slightly northward of the boundary between a north–south-oriented couplet of vertical motion. The robust transverse couplets, first identified 6 h earlier, were still clearly identified in the transverse omega (Fig. 17b). The most intense transverse circulation remained related to quasigeostrophic frontogenesis along the northwest edge of the occluded thermal ridge [in the region of strongest geostrophic winds in the lower to middle troposphere (see Fig. 9b)] and helped to provide strong transverse ascent just north of the surface cyclone. In fact, that ascent maximum accounted for just over 40% of the total QG omega near the cyclone center at this time—a much larger fraction than at any prior time. The majority of the QG omega was still, however, associated with the shearwise component (Fig. 17c). After this time, the QG vertical motions weakened rapidly and development ceased. By 0000 UTC 8 October, the total QG omega was again split about 40/60 between the transverse and shearwise components (not shown).

5. Discussion

Keyser et al. (1992) were among the first to consider a partition of the QG omega into along- and across-isentrope components. They found that the characteristic comma-shaped vertical motion distribution of the

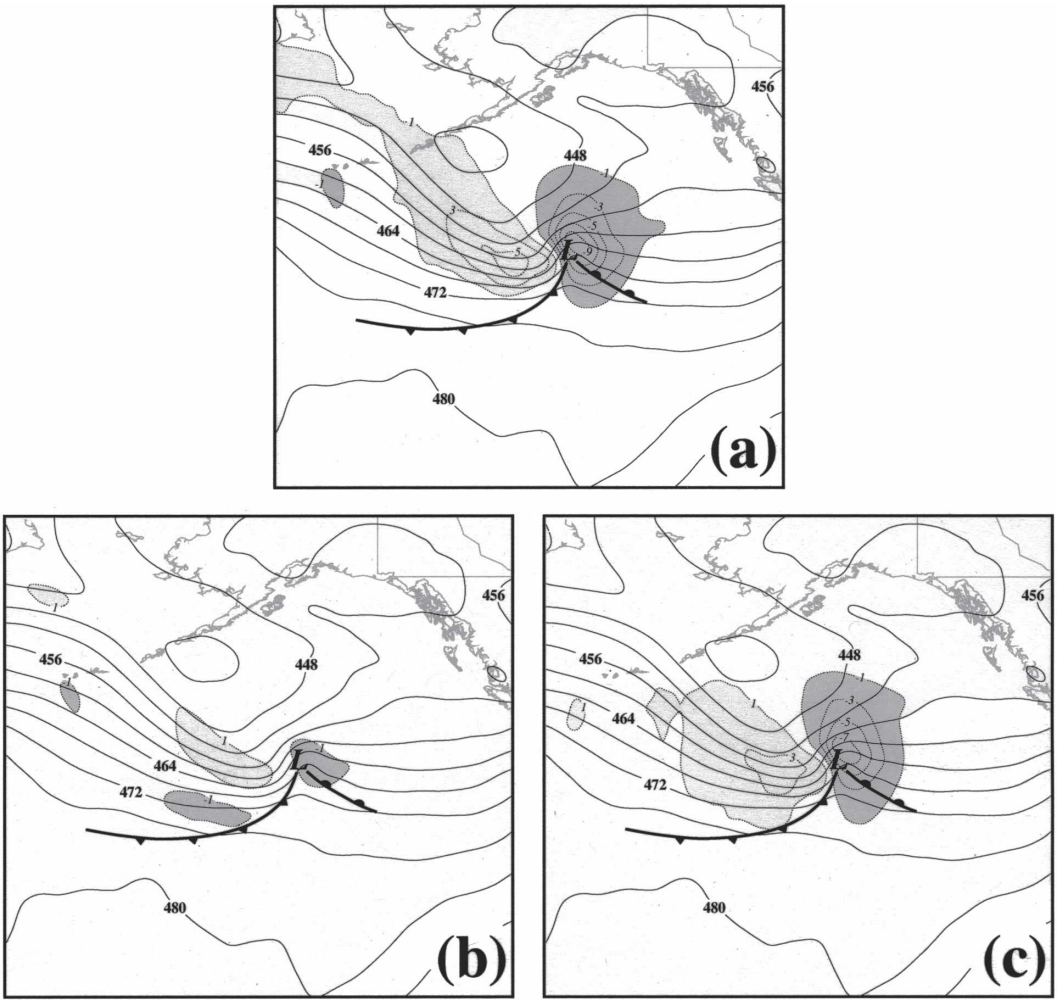

FIG. 15. Same as in Fig. 14, but for 0000 UTC 7 Oct 2004.

midlatitude cyclone resulted from modifications of a cellular dipole pattern in ω, associated with along-isentrope **Q** divergence, by banded dipoles associated with across-isentrope **Q** divergence concentrated near the frontal zones. Their analysis was restricted to the mature and immediate postmature phases of an idealized, primitive equation, channel model cyclone and emphasized the *pattern* separation between the two components of vertical motions rather than their respective physical roles in the cyclone life cycle.

The Keyser et al. (1992) study prompted a number of subsequent efforts that have employed partitioned QG omega diagnostics to investigate a variety of canonical synoptic structures [i.e., cold fronts as in Barnes and Coleman (1993) and occlusions as in Martin (1999a,b)]. To our knowledge, however, the only examinations of observed cyclone life cycles employing a similar partition of the **Q**-vector forcing for omega, prior to the present paper, were those undertaken by Kurz (1992, 1997).[4] In these studies emphasis was placed upon the respective cyclogenetic and frontogenetic processes represented by the partitioned **Q**-vector forcings. Kurz (1992) concluded that a QG frontogenetic circulation often leads to the first stages of lower-tropospheric cyclogenesis but that it must be supported by ascent associated with the passage of an upper-tropospheric shortwave trough in order to sustain development. Careful consideration of the evidence he presents (see his Fig. 8), however, suggests to the author that even the initial cyclogenesis proceeds only when the shearwise forcing for ascent arrives in the vicinity of the surface development. Thus, a plausible alternative interpretation of his evidence is that shearwise ascent

[4] Martin (1999a) examined the $\mathbf{Q}_s/\mathbf{Q}_n$ partition in real cyclones but at only one time. Additionally, Martin (1999b) considered a substantial portion of a cyclone life cycle but only with regard to a further partition of $\mathbf{Q}_s$.

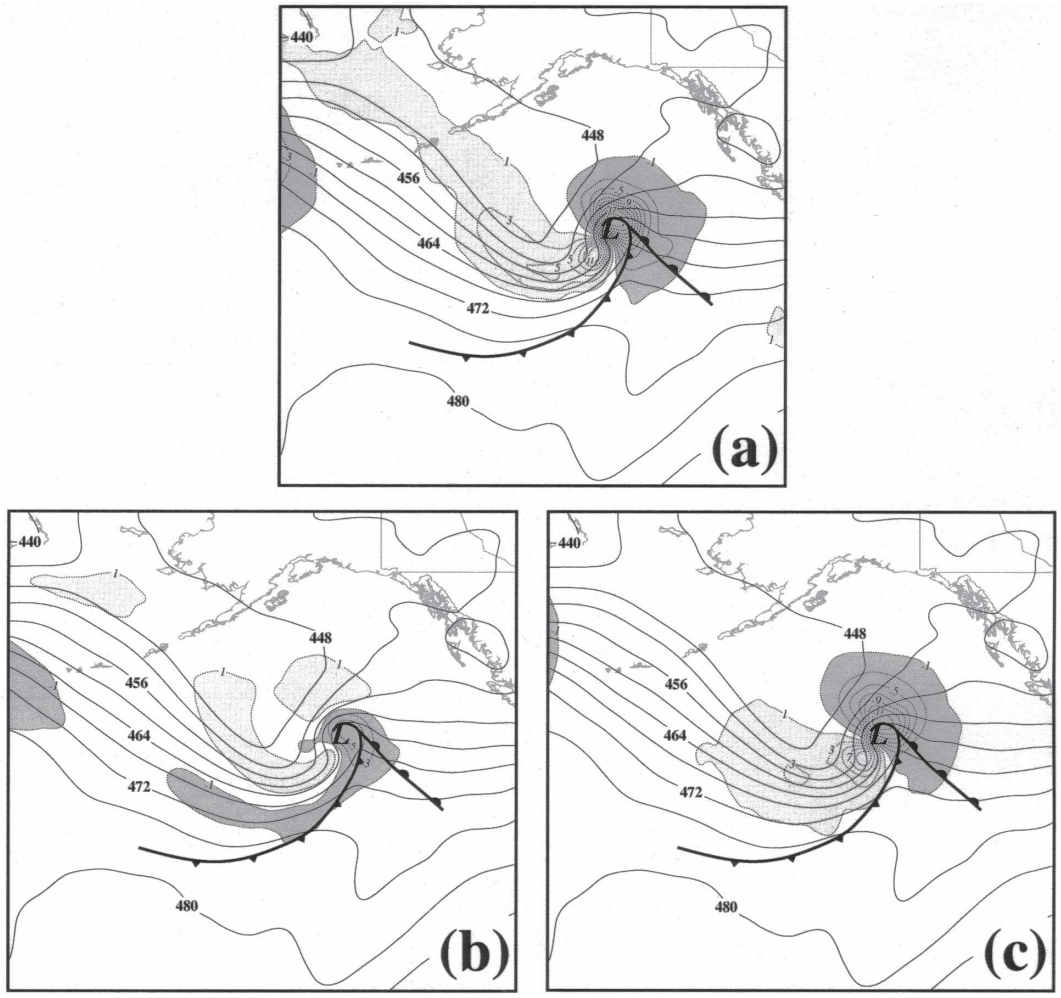

FIG. 16. Same as in Fig. 14, but for 0600 UTC 7 Oct 2004.

dominates the cyclogenesis throughout the development. It is important to note that the Kurz studies show only the *forcing* for QG omega from each component of **Q**, not the actual inverted omega. This can sometimes complicate interpretation in synoptic settings characterized by weak forcing and may underlie the divergence of opinion in this case.

In the present study we have referred to the two components of QG omega as transverse and shearwise, corresponding to those associated with the across- and along-isentrope components of **Q**, respectively. The transverse omega is associated with processes that intensify or weaken $|\nabla\theta|$ (i.e., QG frontogenesis), while the shearwise omega is associated with processes that rotate $\nabla\theta$.

In the foregoing analysis, we have traced the evolutions of the shearwise and transverse vertical motions through the life cycles of two recent Northern Hemisphere surface cyclones. That analysis, as well as the less thorough examination of a large number of other cases (not shown), has suggested the following dynamical picture of the cyclone life cycle. (Other cases are monitored by daily perusal of a Web site on which partitioned QG ω, calculated using NCEP–NCAR model output, is displayed each day; the address for this Web site is http://marrella.aos.wisc.edu/omega/omega.html.) The origin and subsequent intensification of the lower-tropospheric cyclone appears connected to the column stretching and lower-tropospheric vorticity production associated with the updraft portion of the shearwise QG vertical motion, which displays a single, dominant, middle-tropospheric couplet at all stages of the cyclone life cycle. The shearwise ascent is associated with along-isentrope **Q**-vector convergence that is consistent with the simultaneous production of a thermal ridge in the lower troposphere (Martin 1999a). This set of circumstances represents the canonical cyclogenetic environment as described by Hoskins et al. (1985); one char-

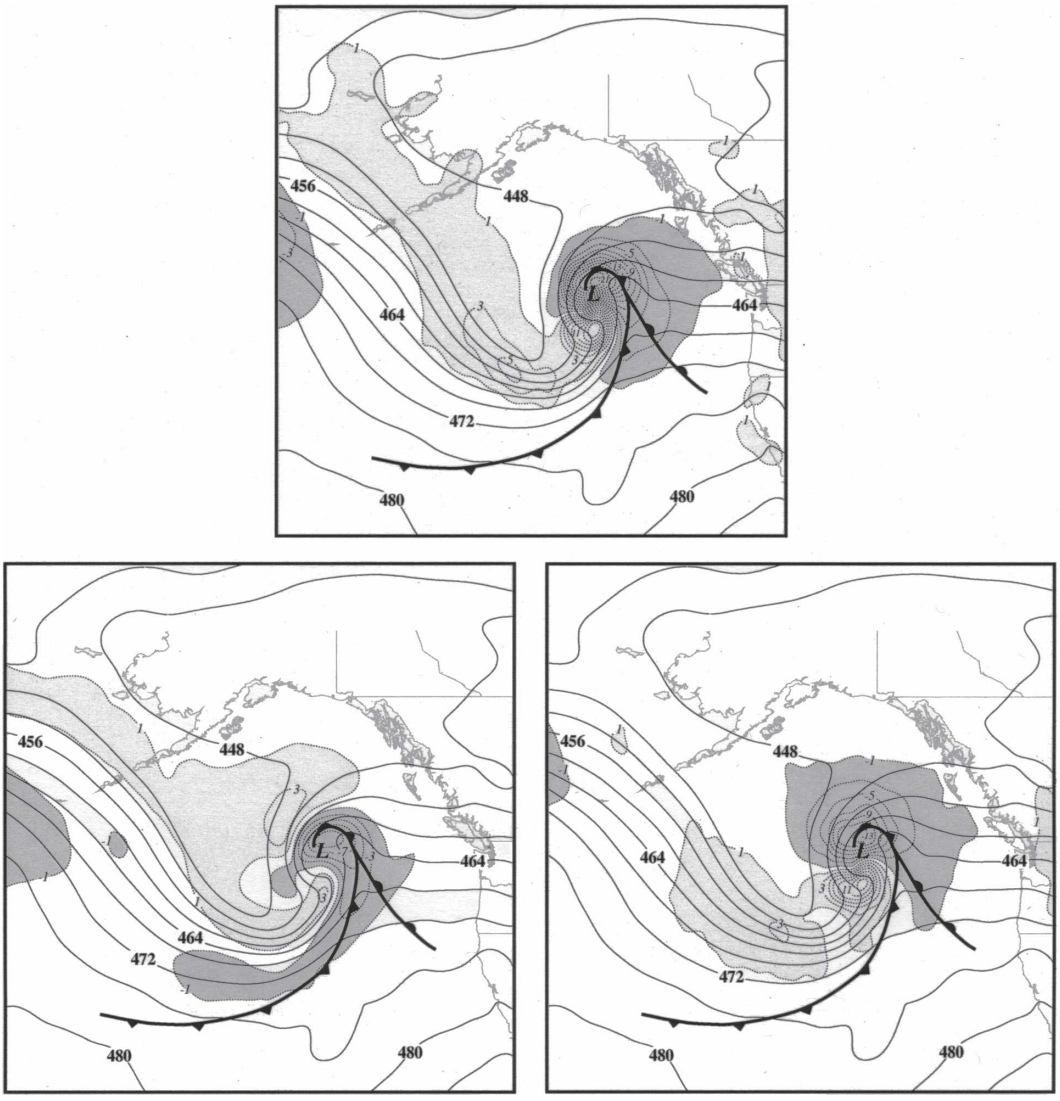

FIG. 17. Same as in Fig. 14, but for 1200 UTC 7 Oct 2004.

acterized by ascent and a lower-tropospheric warm anomaly located downstream of an upper-tropospheric potential vorticity anomaly. It is worth noting that the transverse couplets of vertical motion, unrelated as they are to rotation of $\nabla\theta$, are never associated with the production of such thermal anomalies. This restriction is consistent with the repeated observation that the transverse omega does not play a significant role in the incipient stages of cyclogenesis.

The transverse omega, associated with the frontal zones of the cyclone, appears only after those frontal zones have been established and plays little role in initiating the development of the surface cyclones examined here as a result of the absence of associated local maxima in column stretching near the cyclone center. In fact, less careful examination of a large number of cyclone life cycles over the Northern Hemisphere in the prior winter has revealed no case in which the transverse omega so influences surface cyclogenesis, contrary to the suggestion of Kurz (1992). It does appear, however, that near the end of the mature stage of the life cycle, a transverse response to QG frontogenesis along the western edge of the warm frontal zone (where the geostrophic wind is often very large in the lower troposphere) results in a local maximum of ascent coincident with the shearwise ascent that fuels the continued cyclogenesis (see Figs. 14b, 16b, and 17b). This same signal appeared in a large number of other cases, of varying intensities, in the course of this work and appears, therefore, to be a characteristic aspect of the life cycle.

The present study's persistent lack of evidence for

cyclogenesis events whose initial stages are characterized by dominant transverse QG ascent seems at odds with a large body of prior work concerning the nature of midlatitude cyclogenesis. In their examination of composites of typical surface developments over the North Atlantic Ocean more than 40 yr ago, Petterssen et al. (1962) suggested that surface cyclogenesis comes in two basic types. Formally designated as type A and type B by Petterssen and Smebye (1971), the distinction between these varieties was based upon the two separate forcing terms in the traditional QG omega equation. Type A cyclones were thought to develop in the absence of any significant upper-level disturbance. Correspondingly, the influence of differential vorticity advection (the first term in the traditional QG omega equation) was considered much smaller than the influence of the Laplacian of thermal advection (the second term in the omega equation) in such cases. Type B cyclogenesis occurred when a preexisting upper trough approached a low-level baroclinic zone. In such a case, the influence of vorticity advection overwhelmed that of thermal advection in the initial cyclogenetic stage.

Petterssen et al. (1962) and Petterssen and Smebye (1971) both tacitly assumed that the vorticity advection was most significant at upper-tropospheric levels whereas the influence of thermal advection was largest at lower-tropospheric levels. Deveson et al. (2002) recently noted, however, that the implicit assumption that both thermal advection forcing at upper levels and vorticity advection forcing at lower levels are negligible has never been suitably demonstrated. The resulting emphasis on the *levels* at which these processes occur, inspired by the assumptions made in the seminal works on this topic, has subsequently grown to eclipse an emphasis on the *processes* themselves.

Equally troubling is the fact that these processes, represented by the supposedly separate forcing terms in the traditional QG omega equation, contain considerable internal cancellation as pointed out by Trenberth (1978). The vector frontogenesis approach (Keyser et al. 1988), which considers the across- and along-isentrope components of the **Q** vector, casts this forcing in terms of changes in the magnitude and direction of $\nabla\theta$, respectively, and by so doing places investigation of the relationship between QG omega and the underlying dynamics of midlatitude cyclones on a more physically satisfying foundation. We suggest that the shearwise/transverse perspective on QG omega, coupled with the height attributable diagnostic method of Clough and Davitt (1994) and Clough et al. (1996) may provide new insight by helping to refocus the type A/B debate on physical processes while maintaining a respect for the importance that the vertical distribution of those processes has on cyclogenesis.

The analysis presented here, in conjunction with a large number of cases examined in lesser detail, suggests that, in many cases, cyclogenesis slightly precedes frontogenesis and that the generation of a lower-tropospheric cyclone is initiated by shearwise couplets of vertical motion. We expect that an emphasis on shearwise and transverse vertical motions might be usefully employed to reconsider the physical processes that underlie the development of a number of canonical disturbances in the midlatitude atmosphere including upper-level fronts, documented type A cyclogenesis events [examples of which are included in Petterssen et al. (1962) and Plant et al. (2003)], and jet streak circulations. Future work will pursue investigation of such features from this perspective.

Acknowledgments. This research was supported by a grant from the National Science Foundation (NSF-0202012). Assistance with the computation of QG omega by Dr. Justin McLay is greatly appreciated. Discussions concerning QG omega with Drs. Michael Morgan and Chris Davis are also appreciated. The careful and insightful reviews of Dr. David Schultz, two anonymous reviewers, and Dr. Juan Carlos Jusem are greatly appreciated as well.

REFERENCES

Bader, M. F., G. S. Forbes, J. R. Grant, R. B. E. Lilley, and A. J. Waters, 1995: *Images in Weather Forecasting*. Cambridge University Press, 499 pp.

Barnes, S. L., and B. R. Coleman, 1993: Quasigeostrophic diagnosis of cyclogenesis associated with a cutoff extratropical cyclone—The Christmas 1987 storm. *Mon. Wea. Rev.,* **121,** 1613–1634.

Bjerknes, J., and H. Solberg, 1922: Life cycle of cyclones and the polar front theory of atmospheric circulation. *Geofys. Publ.,* **3,** 1–18.

Clough, S. A., and C. S. A. Davitt, 1994: Development of an Atlantic frontal wave during IOP3 of Fronts92. *The Life Cycles of Extratropical Cyclones,* S. Gronas and M. A. Shapiro, Eds., Vol. 2, Geophysical Institute, University of Bergen, 151–156.

——, ——, and A. J. Thorpe, 1996: Attribution concepts applied to the omega equation. *Quart. J. Roy. Meteor. Soc.,* **122,** 1943–1962.

Deveson, A. C. L., K. A. Browning, and T. D. Hewson, 2002: A classification of FASTEX cyclones using a height-attributable quasi-geostrophic vertical-motion diagnostic. *Quart. J. Roy. Meteor. Soc.,* **128,** 93–117.

Eliassen, A., 1962: On the vertical circulation in frontal zones. *Geofys. Publ.,* **24,** 147–160.

Holton, J. R., 1992: *An Introduction to Dynamical Meteorology*. 3d ed. Academic Press, 511 pp.

Hoskins, B. J., and M. A. Pedder, 1980: The diagnosis of middle latitude synoptic development. *Quart. J. Roy. Meteor. Soc.,* **106,** 707–719.

——, I. Draghici, and H. C. Davies, 1978: A new look at the ω-equation. *Quart. J. Roy. Meteor. Soc.,* **104,** 31–38.

——, M. McIntyre, and A. W. Robertson, 1985: On the use and significance of isentropic potential vorticity maps. *Quart. J. Roy. Meteor. Soc.,* **111,** 877–946.

Keyser, D., M. J. Reeder, and R. J. Reed, 1988: A generalization of Petterssen's frontogenesis function and its relation to the forcing of vertical motion. *Mon. Wea. Rev.,* **116,** 762–780.

——, B. D. Schmidt, and D. G. Duffy, 1992: Quasigeostrophic vertical motions diagnosed from along- and cross-isentrope components of the Q vector. *Mon. Wea. Rev.,* **120,** 731–741.

Kurz, M., 1992: Synoptic diagnosis of frontogenetic and cyclogenetic processes. *Meteor. Atmos. Phys.,* **48,** 77–91.

——, 1997: The role of frontogenetic and frontolytic wind field effects during cyclonic development. *Meteor. Appl.,* **4,** 353–363.

Martin, J. E., 1998: The structure and evolution of a continental winter cyclone. Part I: Frontal structure and the occlusion process. *Mon. Wea. Rev.,* **126,** 303–328.

——, 1999a: Quasigeostrophic forcing of ascent in the occluded sector of cyclones and the trowal airstream. *Mon. Wea. Rev.,* **127,** 70–88.

——, 1999b: The separate roles of geostrophic vorticity and deformation in the midlatitude occlusion process. *Mon. Wea. Rev.,* **127,** 2404–2418.

Petterssen, S., and S. J. Smebye, 1971: On the development of extratropical cyclones. *Quart. J. Roy. Meteor. Soc.,* **97,** 457–482.

——, D. L. Bradbury, and K. Pedersen, 1962: The Norwegian cyclone models in relation to heat and cold sources. *Geofys. Publ.,* **24,** 243–280.

Plant, R. S., G. C. Craig, and S. L. Gray, 2003: On a threefold classification of extratropical cyclogenesis. *Quart. J. Roy. Meteor. Soc.,* **129,** 2989–3012.

Pyle, M. E., D. Keyser, and L. F. Bosart, 2004: A diagnostic study of jet streaks: Kinematic signatures and relationship to coherent tropopanse disturbances. *Mon. Wea. Rev.,* **132,** 297–319.

Reed, R. J., and M. D. Albright, 1986: A case study of explosive cyclogenesis in the eastern Pacific. *Mon. Wea. Rev.,* **114,** 2297–2319.

Sawyer, J. S., 1956: The vertical circulation at meteorological fronts and its relation to frontogenesis. *Proc. Roy. Soc. London,* **A234,** 346–362.

Sutcliffe, R. C., 1947: A contribution to the problem of development. *Quart. J. Roy. Meteor. Soc.,* **73,** 370–383.

Trenberth, K. E., 1978: On the interpretation of the diagnostic quasi-geostrophic omega equation. *Mon. Wea. Rev.,* **106,** 131–137.